

# Comparing simulation of plasma turbulence with experiment.

## II. Gyrokinetic simulations

David W. Ross<sup>a)</sup>

*Fusion Research Center, The University of Texas, Austin, Texas 78712-2068*

William Dorland<sup>b)</sup>

*Imperial College, London, England*

(Received 2 July 2002; accepted 10 September 2002)

The direct quantitative correspondence between theoretical predictions and the measured plasma fluctuations and transport is tested by performing nonlinear gyrokinetic simulations with the GS2 code. This is a continuation of previous work with gyrofluid simulations [D. W. Ross *et al.*, *Phys. Plasmas* **9**, 177 (2002)], and the same L-mode reference discharge in the DIII-D tokamak [J. L. Luxon and L. G. Davis, *Fusion Technol.* **8**, 441 (1985)] is studied. The simulated turbulence is dominated by ion temperature gradient (ITG) modes, corrected by trapped-electron, passing-electron and impurity effects. The energy fluxes obtained in the gyrokinetic simulations are comparable to, even somewhat higher than, those of the earlier work, and the simulated ion thermal transport, corrected for  $\mathbf{E} \times \mathbf{B}$  flow shear, exceeds the experimental value by more than a factor of 2. The simulation also overestimates the density fluctuation level. Varying the local temperature gradient shows a stiff response in the flux and an apparent up-shift from the linear mode threshold [A. M. Dimits *et al.*, *Phys. Plasmas* **7**, 969 (2000)]. This effect is insufficient, within the estimated error, to bring the results into conformity with the experiment. © 2002 American Institute of Physics. [DOI: 10.1063/1.1518997]

### I. INTRODUCTION AND SUMMARY

In the previous work<sup>1</sup> we presented gyrofluid simulations of turbulence and comparison with experiment using the GRYFFIN code. Here we turn to fully nonlinear gyrokinetic simulations of the same L-mode discharge on DIII-D using the GS2 code.<sup>2-6</sup> This code treats both electrons and several species of ions gyrokinetically in a five-dimensional phase space continuum. In particular, trapped and passing electron dynamics and pitch-angle scattering are included. The code is fully electromagnetic,<sup>6,7</sup> but we present only electrostatic examples here. It is a flux tube code, employing magnetic field-line coordinates,<sup>8</sup> and is coupled to an EFIT equilibrium<sup>9</sup> that describes the shaped tokamak geometry. In the range of wave numbers that we consider here ( $k_{\perp} \rho_i \leq 1$ ), the dominant instabilities are ion temperature gradient (ITG) modes, but their growth rates can be strongly modified (usually increased) by the presence of trapped electrons and impurities.

It is expected that the gyrokinetic turbulence levels and associated transport fluxes will be lower than those generated by the gyrofluid code, principally because of improved treatment of zonal flow dynamics. That is, gyrokinetics preserves an undamped component of the zonal flows that suppresses the turbulence.<sup>10</sup> This is especially true near marginal stability, where an effective upshift of the critical temperature gradient, known as the “Dimits shift,”<sup>11</sup> occurs. For our examples, however, the ion temperature gradient is well above

threshold, and the gyrokinetic energy fluxes can exceed those given by the gyrofluid code. One reason for this could lie in the approximations used to represent the trapped particles in the gyrofluid code. (Most benchmarking of the various nonlinear codes has been carried out with adiabatic electrons.<sup>11</sup> In that limit for our example the gyrofluid and gyrokinetic codes agree fairly closely.)

Varying the input ion temperature gradient we do see a “stiffer” response and evidence of a Dimits shift in the gyrokinetic results. However, just as in the gyrofluid case the results remain larger than the experimental values for any temperature gradient that is consistent with the experimental values within the uncertainties of the measurement. We describe the GS2 code and its properties in Sec. II, and briefly review the experimental data. (The paper is meant to be read in conjunction with Ref. 1.) In Sec. III we compare the simulations with the data and with the previous simulations, and in Sec. IV we reflect on the results and speculate on how they might be improved.

### II. THE CODE, SIMULATION OUTPUT, AND EXPERIMENTAL DATA

GS2 is a nonlinear gyrokinetic code that computes turbulence in a flux tube centered at the chosen radius.<sup>2-6</sup> It makes use of ballooning formalism, taking the sheared magnetic geometry from an EFIT equilibrium.<sup>9</sup> Input consists of fixed background values and gradients that are experimentally determined, and grid and mode distributions commensurate with the expected dominant turbulence. In five-dimensional phase space the code calculates the evolution of a main ion species, one or more impurity species, and elec-

<sup>a)</sup>Electronic mail: dwross@mail.utexas.edu

<sup>b)</sup>Present address: The University of Maryland.

trons on drift-wave time scales. The electron response includes nonadiabatic trapped- and passing-electron contributions. Thus, transport of both energy and particles is calculated, and trapped electron modes and impurity drift waves are included along with their coupling, both linearly and nonlinearly, to the ITG modes.

The code is fully electromagnetic,<sup>6</sup> but the calculations presented here are electrostatic, i.e.,  $\tilde{A}_{\parallel} = \tilde{A}_{\perp} = 0$ . Electromagnetic results, which require much more computer time, have been reported<sup>6,7</sup> and will be discussed more fully elsewhere.<sup>12</sup> At the low values of  $\beta = 2\mu_0 nT/B^2$  in this discharge, we expect the electromagnetic effects to be small. The linear growth rates for the present case are, in fact, reduced by a small amount (which we judge to be inconsequential) from the electrostatic ones. In nonlinear electromagnetic simulations of other discharges,<sup>7</sup> we have found that the electrostatic energy fluxes  $Q_j^{\text{es}} = 3\langle \tilde{p}_j \tilde{v}_E \rangle / 2$  are not significantly changed, nor is there a significant contribution to the electromagnetic ion energy flux  $Q_i^{\text{em}} = \langle \tilde{q}_{i\parallel} \tilde{B}_r \rangle / B_0$ . We have observed, however, a modest but theoretically interesting contribution in the electron channel from  $Q_e^{\text{em}} = \langle \tilde{q}_{e\parallel} \tilde{B}_r \rangle / B_0$ . This effect, which is still under investigation, would not improve the results of the present paper.

A principal saturation mechanism, which is accounted for by the code, arises from the toroidally and poloidally symmetric modes, i.e., the zonal flows.<sup>13</sup> Background  $\mathbf{E} \times \mathbf{B}$  flow shear, however, is not included, nor are equilibrium gradient variations across the computational domain.<sup>14</sup>

Other features of the code input are similar to those of the gyrofluid code reported previously, except that the mid-plane half-diameter  $a$  replaces the density gradient scale length  $L_{ne}$  in the normalizations, where  $L_{ne} = a(dn_e/d\rho)^{-1}$ , and  $\rho$  is the normalized flux-surface label. For example, the energy fluxes are normalized to  $n_e T_i \rho_i^2 v_{Ti}^2 / a^2$  rather than  $n_e T_i \rho_i^2 v_{Ti}^2 / L_{ne}^2$ , where  $v_{Ti} = \sqrt{T_i/m_i}$  and  $\rho_i = v_{Ti}/\omega_{ci}$ . The cases presented here were run with 11 poloidal modes (with  $k_{\theta}\rho_i \leq 1.0$ ) and 39 radial modes on 429 processors of the T3E (MCURIE) at the National Energy Research Scientific Computing Center (NERSC). A typical run required about 5.7 hours per processor to calculate 9000 time steps.

We believe the poloidal and radial box size and resolution are adequate to describe the ITG modes. The poloidal wave number spectrum is smooth, peaks at about  $k_{\theta}\rho_i = 0.35$ , and should be well covered by 11 modes with  $k_{\theta}\rho_i \leq 1.0$ . This does not preclude interaction with higher wave number electron modes, which we do not investigate here. The radial mode distribution and box size are chosen as in the GRYFFIN code, to achieve higher radial mode numbers for higher  $k_{\theta}\rho_i$  in the ballooning representation, i.e.,  $k_r = \hat{s}k_{\theta}$ . Resolution studies by Mikkelsen<sup>15</sup> support our choices, and will be reported elsewhere.

We compare with the same data described in Ref. 1: energy fluxes derived from a TRANSP<sup>16</sup> analysis and density fluctuations from BES measurements<sup>17</sup> on shot 98777 in DIII-D. This is a reference L-mode discharge used for comparison with a neon injection experiment.<sup>18–21</sup> Here, in Table I, we repeat only a portion of Table I of Ref. 1 showing the

TABLE I. Experimental transport losses through the surface  $\rho=0.7$  at  $t = 1160$  ms of the reference shot, 98777. Here,  $A = 37.6 \text{ m}^2$  is the area of the flux surface.

Energy fluxes	Loss through surface MW
Ion thermal conduction	$q_i A = 1.3$
Ion thermal convection	$\frac{3}{2} \Gamma_i T_i A = 0.2$
Total ion thermal flux	$Q_i A = q_i A + \frac{3}{2} \Gamma_i T_i A = 1.5$
Electron thermal conduction	$q_e A = 1.2$
Electron thermal convection	$\frac{3}{2} \Gamma_e T_e A = 0.2$
Total electron thermal flux	$Q_e A = q_e A + \frac{3}{2} \Gamma_e T_e A = 1.4$
Total thermal flux	$(Q_e + Q_i) A = 2.9$

total electron and ion energy losses,  $P_j = Q_j A$ , through the radial position  $\rho=0.7$ , where  $Q_j$  is the flux and  $A$  is the surface area.

The density fluctuation level estimate of Ref. 1 at this radius is  $|\tilde{n}/n| \leq 0.4\%$  to  $|\tilde{n}/n| \leq 0.6\%$ .

### III. SIMULATION RESULTS AND COMPARISON WITH DATA

Figure 1 shows the time dependence of the total ion (including impurities) and electron transport fluxes, presented in dimensional units as total energy (MW) crossing the surface at  $\rho=0.7$  vs time ( $\mu\text{s}$ ). After the initial transient, the transport settles down to a near steady state with fluctuations and occasional bursts. The average values,  $P_i + P_{\text{imp}} = 4.9 \text{ MW}$  and  $P_e = 3.8 \text{ MW}$  exceed the observed experimental values listed in Table I by factors 3.3 and 2.7, respectively. Figure 2 shows the normalized potential fluctuation spectrum as a function of the normalized poloidal wave number  $k_{\theta}\rho_i$  (omitting the  $k_{\theta}\rho_i = 0$  component, which represents the zonal flows). This resembles both the experimental and the simulated-gyrofluid density fluctuation spectra shown in Figs. 5 and 6 of Ref. 1, respectively, but shifted to slightly lower wave number.

To investigate the stiffness of the response to the ion temperature gradient, we varied  $dT_i/d\rho$ , while holding  $dT_e/d\rho$  fixed. The resulting dependence is compared with that of the gyrofluid results of Ref. 1 and to the maximum normalized linear growth rate in Fig. 3. Plotted against

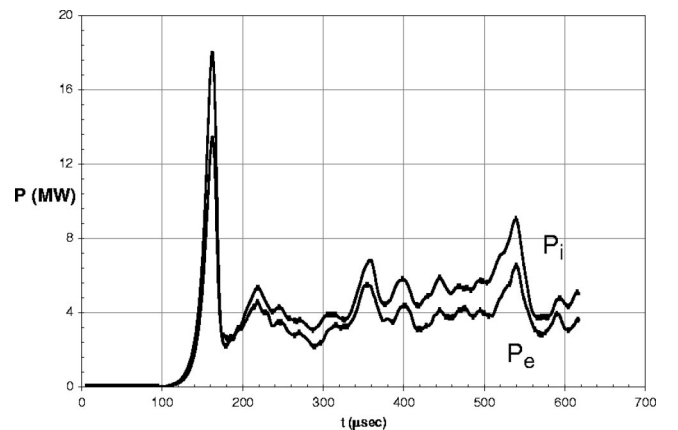


FIG. 1. Electron and total ion energy flow through  $\rho=0.7$ .

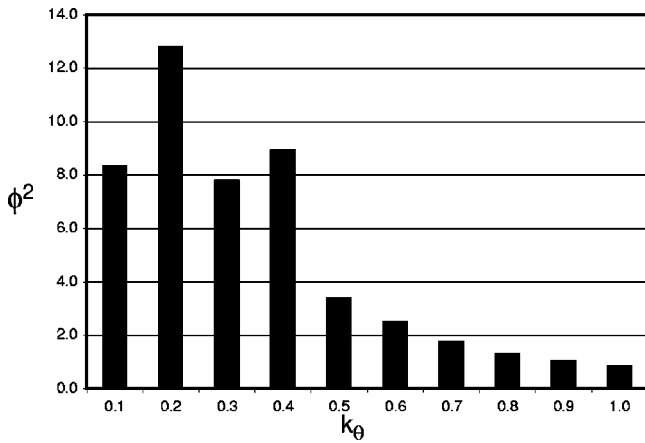


FIG. 2. Potential fluctuation spectrum vs normalized poloidal wave number, omitting the axisymmetric (zonal flow) component.

$R/L_{Ti}$ , the gyrokinetic power flux is steeper, i.e., “stiffer,” than either the growth rate or the gyrofluid result, both of which tend toward the same threshold as the gradient decreases. Thus, there is evidence for the “Dimitis shift” in the gyrokinetic simulation. Interestingly, the GS2 result is actually higher than the gyrofluid one at the nominal gradient value. This may be in part a linear effect, owing to the different treatment of electron dynamics. With both trapped and passing electrons and a more accurate treatment of the trapped electrons, the GS2 code yields somewhat larger linear growth rates than GRYFFIN. The real frequencies are in good agreement between the codes, as are the growth rates with adiabatic electrons. In nonlinear runs with adiabatic electrons GRYFFIN yields  $P_i + P_{imp} = 2.4$  MW, while the GS2 result is  $P_i + P_{imp} = 2.0$  MW. Both results are closer to the experimental value than those obtained with the complete electron dynamics, and the gyrofluid result is the larger of the two as expected from earlier work.<sup>11</sup>

To take into account the equilibrium  $\mathbf{E} \times \mathbf{B}$  flow shear, we apply the “quench rule” of Waltz *et al.*<sup>22</sup> in the same way as in Ref. 1, that is we multiply the power flux by  $(1 - \omega_E/\gamma_{max})$ , where  $\omega_E$  is the shear rate. Here, again evaluating the Hahn–Burrell shear frequency as  $\omega_E = 2.5 \times 10^4$  s<sup>-1</sup> and the Waltz *et al.* value as  $\omega_E = 9.7 \times 10^3$  s<sup>-1</sup>,

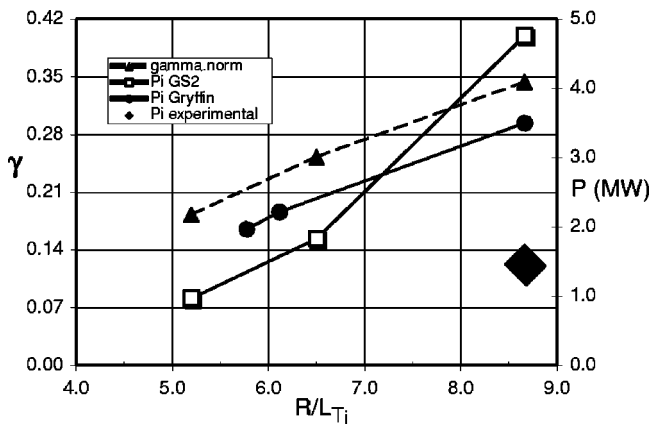


FIG. 3. Ion energy flow vs temperature gradient, compared with the gyrofluid result, the experimental value, and the normalized linear growth rate.

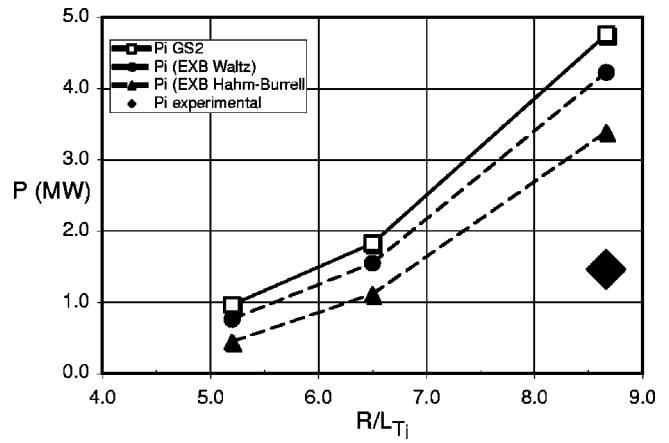


FIG. 4. Ion energy flow vs ion temperature gradient, with and without “quench rules.”

and using the GS2 maximum growth rate at the nominal temperature gradient of  $\gamma_{max} = 8.7 \times 10^4$  s<sup>-1</sup> (corrected as the temperature gradient varies), we plot the estimates of the corrected energy flux in Fig. 4, together with the experimentally measured value vs  $R/L_{Ti}$ . To reconcile the simulations with the experiment, we must choose a temperature gradient between 65% and 75% of the nominal value. Recall that we have deliberately chosen a plasma radius where the measured flow shear is small.<sup>1</sup> At other radii  $\omega_E$  is significantly larger, since this a relatively low field ( $B = 1.6$  T) and therefore high  $\rho_*$  ( $\rho_*^{-1} \sim 120$ ) discharge.

To infer that the simulation results are not within the experimental error, we first invoke the assumption that the experimental profiles are smooth. This is done in most transport analyses. If it were not so, then our theoretical comparisons would be even more difficult. Since the ITG modes in our simulation are well above threshold, the nonlinear fluxes must be smooth functions of the variables. Therefore, if we were to compute the fluxes at multiple radii, using the nominal plasma profiles, we would consistently be high in our estimates. On the other hand, if we were to flatten the local profiles at  $\rho = 0.7$ , within the error estimates of the local gradients, we could achieve agreement with the measured fluxes at that radius.<sup>5</sup> This would require the profiles to be steeper at a nearby radial location to be consistent with the global profile, which would in turn require one to recalculate the profile of  $\omega_E$ . Because  $\omega_E$  is a sensitive function of the profile shape, it is difficult to conclude with certainty that the experimental data would be inconsistent with simulations that included  $\omega_E$  physics directly. Moreover, the simulation results also depend on other parameters, e.g., the magnetic shear and safety factor,  $\hat{s}$  and  $q$ , which are also uncertain. We have not completely ruled out the possibility of generally improving the fit. A full study of these variations, like the one begun by Mikkelsen *et al.* for Alcator C-Mod discharges,<sup>23</sup> will be presented in a future publication. Because of the potential importance of  $\omega_E$  physics, a similar analysis with a global or flux-ribbon (finite annulus) code may ultimately be required for large  $\rho_*$  cases like this.

Finally, at the nominal temperature gradient, we estimate the gyrokinetic density fluctuation level as  $|\bar{n}_e/n_e| = 1.5\%$ ,

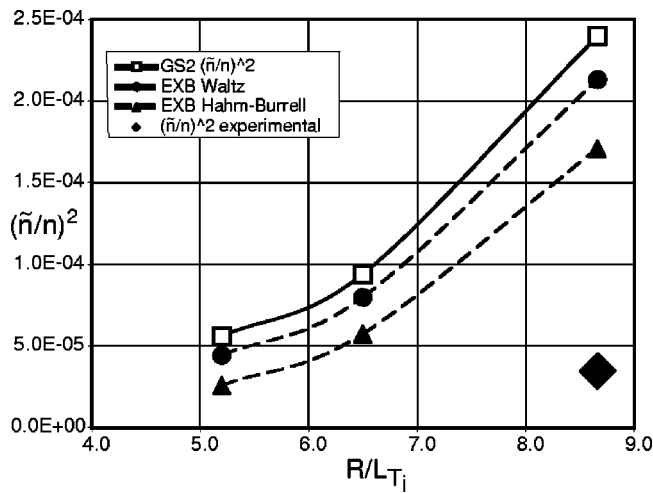


FIG. 5. Electron density fluctuations vs ion temperature gradient, with and without “quench rules.”

roughly 3.0 times that of the experiment. Since we expect (and observe in the simulations) that the transport fluxes vary as  $|\tilde{n}_e/n_e|^2$ , this discrepancy is much larger than that of the transport. Even arguing that a smaller temperature gradient within the error bars could reconcile the energy fluxes we would be left with a fluctuation-amplitude discrepancy. This is illustrated in Fig. 5, where we plot  $|\tilde{n}_e/n_e|^2$  against  $R/L_{Ti}$  as in Fig. 4, together with the much smaller experimental value.

#### IV. CONCLUSIONS AND DISCUSSION

Carrying out gyrokinetic simulations of ITG turbulence in realistic geometry with full electron dynamics at  $\rho=0.7$  for a DIII-D discharge, we find that the values of the electron and ion energy losses,  $P_e$  and  $P_i+P_{imp}$ , and the perturbed density fluctuation level  $|\tilde{n}_e/n_e|$ , exceed the experimental values by factors of 2.7, 3.3, and 3.0, respectively. Having chosen a radius where  $\mathbf{E}\times\mathbf{B}$  flow shear is relatively small we cannot correct these discrepancies by applying a simple quench rule, nor, assuming smooth profiles, can we resolve them by assuming a smaller temperature gradient within the error estimates.

The discussion of Sec. V of Ref. 1 continues to apply and we will not repeat it here. Despite our inability to match the experiment by applying the quench rule, the most likely explanation of the discrepancies is nonlocal behavior owing to variations of the plasma gradients. We speculate that modes can be coupled to neighboring regions where the flow-shear effect is larger. Recent progress has been made on this issue, with signs of reduced fluxes appearing in a flux-ribbon code.<sup>14,24,25</sup> It is also possible that direct coupling to short wavelength ETG turbulence may be partly responsible for the discrepancies we find. We speculate that ETG modes could be excited by the gradients of electron temperature fluctuations associated with the nonadiabatic trapped electrons. Because ETG modes can produce large thermal diffusion,<sup>3</sup> it is possible that such secondary excitations would significantly reduce the nonadiabatic electron component of the ITG turbulence. We note that ITG simulations

which assume an adiabatic electron response are in considerably better agreement with the experimental data. Nonlinear simulations which include this physics directly will be reported elsewhere. In either case, further tests and benchmarking are required to determine whether these particular experimental results can be reproduced with first principles simulations.

#### ACKNOWLEDGMENTS

We wish to thank R. V. Bravenec, G. R. McKee, R. J. Fonck, M. Murakami, K. H. Burrell, G. L. Jackson, G. M. Staebler, R. E. Waltz, W. M. Nevins, and F. Jenko for supplying data and for helpful discussions.

This work is supported by USDOE Grant No. DE-FG03-95ER54296. Our studies are part of the Numerical Tokamak Turbulence Project (NTTP). We have used resources of the National Energy Research Scientific Computing Center, which is supported by the Office of Science of the U.S. Department of Energy under Contract No. DE-AC03-76SF00098.

- <sup>1</sup>D. W. Ross, R. V. Bravenec, W. Dorland, M. A. Beer, G. W. Hammett, G. R. McKee, R. J. Fonck, M. Murakami, K. H. Burrell, G. L. Jackson, and G. M. Staebler, *Phys. Plasmas* **9**, 177 (2002).
- <sup>2</sup>M. Kotschenreuther, G. Rewoldt, and W. M. Tang, *Comput. Phys. Commun.* **88**, 128 (1995).
- <sup>3</sup>W. Dorland, F. Jenko, M. Kotschenreuther, and B. N. Rogers, *Phys. Rev. Lett.* **85**, 5579 (2000).
- <sup>4</sup>F. Jenko, W. Dorland, M. Kotschenreuther, and B. N. Rogers, *Phys. Plasmas* **7**, 1904 (2000).
- <sup>5</sup>W. Dorland, B. N. Rogers, F. Jenko, M. Kotschenreuther, G. W. Hammett, D. Mikkelsen, D. W. Ross, M. A. Beer, P. B. Snyder, R. Bravenec, M. Greenwald, D. Ernst, and R. Budny, *Fusion Energy 2000* (International Atomic Energy Agency, Vienna, 2000).
- <sup>6</sup>F. Jenko and W. Dorland, *Plasma Phys. Controlled Fusion* **43**, A141 (2001).
- <sup>7</sup>D. W. Ross, W. Dorland, and B. N. Rogers, *Bull. Am. Phys. Soc.* **46**, 115 (2001).
- <sup>8</sup>M. A. Beer, S. C. Cowley, and G. W. Hammett, *Phys. Plasmas* **2**, 2687 (1995).
- <sup>9</sup>L. L. Lao, H. St. John, R. D. Stambaugh, A. G. Kellman, and W. Pfeiffer, *Nucl. Fusion* **25**, 1611 (1985).
- <sup>10</sup>M. N. Rosenbluth and F. L. Hinton, *Phys. Rev. Lett.* **80**, 724 (1998).
- <sup>11</sup>A. M. Dimits, G. Bateman, M. A. Beer, B. I. Cohen, W. Dorland, G. W. Hammett, C. Kim, J. E. Kinsey, M. Kotschenreuther, A. H. Kriz, L. L. Lao, J. Mandrekas, W. M. Nevins, S. E. Parker, A. J. Redd, D. E. Shumaker, R. Sydora, and J. Weiland, *Phys. Plasmas* **7**, 969 (2000).
- <sup>12</sup>D. W. Ross, W. Dorland, and B. N. Rogers, “Electromagnetic gyrokinetic simulations of tokamak microturbulence,” *Phys. Plasmas* (to be submitted).
- <sup>13</sup>G. W. Hammett, M. A. Beer, W. Dorland, S. C. Cowley, and S. A. Smith, *Plasma Phys. Controlled Fusion* **35**, 973 (1993).
- <sup>14</sup>R. E. Waltz, J. M. Candy, and M. N. Rosenbluth, *Phys. Plasmas* **9**, 1938 (2002).
- <sup>15</sup>D. Mikkelsen (private communication).
- <sup>16</sup>R. J. Hawryluk, in *Physics of Plasmas Close to Thermonuclear Conditions*, edited by B. Coppi, G. G. Leotta, D. Pfirsch, R. Pozzoli, and E. Sindoni (Pergamon, Oxford, 1980), Vol. 1, p. 19 (see also <http://w3.pppl.gov/transp/>).
- <sup>17</sup>R. J. Fonck, N. Bretz, G. Cosby, R. Durst, E. Mazzucato, R. Nazikian, S. Paul, S. Scott, W. Tang, and M. Zarnstorff, *Plasma Phys. Controlled Fusion* **34**, 1903 (1992).
- <sup>18</sup>G. R. McKee, M. Murakami, J. A. Boedo, N. H. Brooks, K. H. Burrell, D. Ernst, R. J. Fonck, G. L. Jackson, M. Jakubowski, R. J. LaHaye, A. M. Messiaen, J. Ongena, C. L. Rettig, B. Rice, C. Rost, G. M. Staebler, R. Sydora, D. M. Thomas, B. Unterberg, M. R. Wade, and W. P. West, *Phys. Plasmas* **7**, 1870 (2000).
- <sup>19</sup>M. Murakami, G. R. McKee, G. L. Jackson, G. M. Staebler, D. A. Alex-

- ander, D. R. Baker, G. Bateman, L. R. Baylor, J. A. Baedo, N. H. Brooks, K. H. Burrell, J. R. Cary, R. H. Cohen, R. J. Colchin, J. C. DeBoo, E. J. Doyle, D. R. Ernst, T. E. Evans, C. Fenzi, C. M. Greenfield, D. E. Greenwood, R. J. Groebner, J. T. Hogan, W. A. Houlberg, A. M. Hyatt, R. Jayakumar, T. C. Jornigan, R. A. Jong, J. E. Kinsey, A. H. Kritz, R. J. La Haye, L. L. Lao, C. J. Lasnier, M. A. Makowski, J. Mandrekas, A. M. Messiaen, R. A. Moyer, J. Ongena, A. Pankin, T. W. Petrie, C. C. Petty, C. L. Rettig, T. L. Rhodes, B. W. Rice, D. W. Ross, J. C. Rost, S. G. Shasharina, H. E. St John, W. M. Stacey, P. I. Strand, R. D. Sydora, T. S. Taylor, D. M. Thomas, M. R. Wade, R. E. Waltz, W. P. West, K. L. Wong, and L. Zeng, *Nucl. Fusion* **41**, 317 (2001).
- <sup>20</sup>M. Murakami, G. L. Jackson, G. R. McKee, C. L. Rettig, G. M. Staebler, D. R. Baker, J. A. Boedo, N. H. Brooks, K. H. Burrell, D. R. Ernst, T. E. Evans, R. J. Fonck, C. M. Greenfield, J. E. Kinsey, L. L. Lao, M. A. Makowski, A. Messiaen, J. Mandrekas, J. Ongena, G. Rewoldt, B. W. Rice, D. W. Ross, H. E. St John, R. Sydora, D. M. Thomas, B. Untenberg, M. R. Wade, W. P. West, K. L. Wong, and D.-D. Team, *Fusion Energy 2000* (International Atomic Energy Agency, Vienna, 2000).
- <sup>21</sup>M. Murakami, G. R. McKee, G. L. Jackson, G. M. Staebler, D. R. Baker, J. A. Boedo, N. H. Brooks, K. H. Burrell, D. R. Ernst, T. E. Evans, C. M. Greenfield, R. J. Groebner, J. E. Kinsey, R. J. La Haye, L. L. Lao, A. Messiaen, J. Mandrekas, J. Ongena, C. L. Rettig, B. W. Rice, D. W. Ross, H. E. St John, R. D. Sydora, D. M. Thomas, M. R. Wade, W. P. West, and DIII-D Team, *Proceedings of the 26th European Conference on Controlled Fusion and Plasma Physics* (The European Physical Society, Petit-Lancy, 2000).
- <sup>22</sup>R. E. Waltz, R. L. Dewar, and X. Garbet, *Phys. Plasmas* **5**, 1784 (1998).
- <sup>23</sup>D. Mikkelsen, G. Taylor, W. Dorland, D. W. Ross, M. Greenwald, C. Fiore, A. Hubbard, J. Irby, E. Marmor, D. Messiaen, J. Rice, J. Terry, and S. Wolfe, *Bull. Am. Phys. Soc.* **46**, 115 (2001).
- <sup>24</sup>J. Candy, R. E. Waltz, and M. N. Rosenbluth, *Proceedings of the 28th European Conference on Controlled Fusion and Plasma Physics, Madeira, Portugal* (The European Physical Society, Petit-Lancy, 2001), paper P2.054 (published on a CD-ROM).
- <sup>25</sup>J. Candy and R. E. Waltz "An Eulerian gyrokinetic Maxwell solver," *J. Comput. Phys.* (submitted).